Electrophysiological and molecular identification of voltage-gated sodium channels in murine vascular myocytes

Sohag Saleh, Shuk Yin M. Yeung, Sally Prestwich, Vladimír Pucovský and Iain Greenwood

Division of Basic Medical Sciences, St George's, University of London, London SW17 0RE, UK

A voltage-gated Na^+ current was characterised in freshly dissociated mouse portal vein (PV) smooth muscle myocytes. The current was found superimposed upon the relatively slow L-type Ca^{2+} current and was resistant to conventional Ca^{2+} channel blockers but was abolished by external Na^+ replacement and tetrodotoxin (TTX, 1 μM). The molecular identity of the channel responsible for this conductance was determined by RT-PCR where only the transcripts for Na^+ channel genes *SCN7a*, *8a* and *9a* were detected. The presence of the protein counterparts to the *SCN8a* and *9a* genes ($NaV_{1.6}$ and $NaV_{1.7}$, respectively) on the individual smooth muscle myocytes were confirmed in immunocytochemistry, which showed diffuse staining around a predominantly plasmalemmal location. TTX inhibited the action potential in individual myocytes generated in the current clamp mode but isometric tissue tension experiments revealed that TTX (1 and 5 μM) had no effect on the inherent mouse PV rhythmicity. However, the Na^+ channel opener veratridine (10 and 50 μM) significantly increased the length of contraction and the interval between contractions. This effect was not influenced by pre-incubation with atropine, prazosin and propranolol, but was reversed by TTX (1 μM) and completely abolished by nicardipine (1 μM). Furthermore, preincubation with the reverse-mode Na^+–Ca^{2+} exchange blocker KB-R7943 (10 μM) also inhibited the veratridine response. We have established for the first time the molecular identity of the voltage-gated Na^+ channel in freshly dispersed smooth muscle cells and have shown that these channels can modulate contractility through a novel mechanism of action possibly involving reverse mode Na^+–Ca^{2+} exchange.

(Received 19 May 2005; accepted after revision 13 July 2005; first published online 14 July 2005)
Corresponding author I. Greenwood: Division of Basic Medical Sciences, St George's, University of London, London SW17 0RE, UK. Email: i.greenwood@sgul.ac.uk

Voltage-gated sodium (Na^+) channels (VGSCs) are involved in the generation and propagation of action potentials along nerve fibres. They are also important components of skeletal muscle and cardiac muscle action potentials. In general voltage-gated Na^+ currents activate rapidly upon membrane depolarization and then inactivate rapidly and can be subdivided by their relative sensitivity to tetrodotoxin (TTX). To date 11 genes (*SCNa1–11*) have been identified that encode for TTX-sensitive and TTX-insensitive Na^+ channels and the expression of these genes is highly dependent upon the cell type (Ogata & Ohishi, 2002).

In contrast to their established role in neurones, cardiomyocytes and skeletal muscle cells, voltage-gated Na^+ channels are not thought to play a role in the contractility of smooth muscle, where membrane depolarization and any subsequent contraction are principally governed by the opening of voltage-dependent Ca^{2+} channels (VDCCs). Whilst there has been no convincing evidence to contradict this view, there are a number of electrophysiological studies that show that voltage-gated Na^+ currents are present in smooth muscle cells (SMCs) including rat myometrium (Amédée *et al.* 1986), rat portal vein (Mironneau *et al.* 1990), neonatal azygous vein (Sturek & Hermsmeyer, 1986), guinea pig ureter (Muraki *et al.* 1991), sheep lymphatics (Hollywood *et al.* 1997) and rat vas deferens (Belevych *et al.* 1999). However, the paucity of studies on this conductance in SMCs means that there is little information on its functional role. Moreover, the genes responsible for the Na^+ currents have only been determined in cultured cells (Deshpande *et al.* 2002; Jo *et al.* 2004) or freshly dispersed human jejunal myocytes isolated from morbidly obese individuals (Holm *et al.* 2002; Ou *et al.* 2002). In jejunal smooth muscle cells the Na^+ current was relatively insensitive to TTX and therefore only the expression of genes that encode TTX-insensitive

 DOI: 10.1113/jphysiol.2005.090951

Table 1. Nucleotide sequences for the custom designed primers used to detect the Na^+ channel gene isoforms in RT-PCR

Gene name	REFseq ID	Primer sequence (5′-to 3′)	Gene name	REFseq ID	Primer sequence (5′-to 3′)
SCN1a	AJ810505	F- AGCCTCACTGTGACTGTGCC R- CTATTCGGAAGCACGTCCTCC	*SCN8a*	NM_011323	F- GGGAGGACGATGAAGACAG R- TCAGGCAGAACACCGTCAG
SCN3a	NM_018732	F- CAACGAGGACTGCAAGCTC R- GCTTTTCGGAAGCACTCCC	*SCN9a*	XM_196271	F- CAGCAAAGAGAGACGGAACC R- CCCTCAGTGTCCGTAGAGATT
SCN4a	NM_133199	F- CATCAAATCCCTGCGCACGC R- ATAAAGATGACGAAGTAAAGG	*SCN10a*	NM_009134	F- CAGCGCAGGATGTCCTTCC R- CGGCTTGGAGCATGGCATC
SCN5a	NM_021544	F- CAGGTCGGAAACCTGGTCTTCAG R- GGAGCTGAGCAGCAAGGCCAAGAAG	*SCN11a*	NM_011887	F- TCCCAGGAGCCTTGTTTCCC R- CAGCACTCTGAGGGAAGCC
SCN7a	NM_009135	F- TGCTTCAGGAGAATCTGATATAG R- CAGAATCAATTGCTGAATTCATAA	β-Actin		F- GGCTACAGTTTCACCACCAC R- ACTCCTGCTTGCTGATCCAC

channels (*SCN5a*, *10a* and *11a*) were tested. In the studies on cultured cells the Na^+ currents were TTX sensitive and in the oesophageal myocytes this was due to expression of *SCN4a* and *SCN6a* (Deshpande *et al.* 2002; Jo *et al.* 2004). In contrast, Jo *et al.* (2004) failed to detect either *SCN4a* or *SCN6a* in cultured myocytes from pulmonary and coronary artery but proposed that the major gene whose expression is responsible for the TTX-sensitive current in these cells was *SCN9a*. Maintaining cells under culture conditions may not reflect the physiological scenario in freshly dispersed myocytes. Consequently, there is a need to determine the full expression profile of all *SCNa* genes in freshly dispersed myocytes from normal, healthy tissue.

Recent work in our laboratory aimed at characterising calcium-activated chloride currents ($I_{Cl(Ca)}$) in murine portal vein myocytes revealed the existence of a rapidly activating inward current in a number of cells that was superimposed upon a dihydropyridine-sensitive calcium current (Saleh & Greenwood, 2005). The aim of the present body of work was to characterise completely the fast inward current and to investigate the functional role and molecular characteristics of this conductance. We provide evidence for not only the expression of the Na^+ channel gene isoforms *SCN8a* and *SCN9a* but also for the existence of their respective channel protein correlates ($NaV_{1.6}$ and $NaV_{1.7}$). Moreover, we reveal that activation of voltage-gated Na^+ channels enhances portal vein contractility possibly via reverse mode Na^+–Ca^{2+} exchange. Preliminary results have been communicated to the Physiological Society (Saleh & Greenwood, 2003).

Methods

Tissue retrieval and electrophysiology

Female BALB/c mice (6–8 weeks) were killed by cervical dislocation in accordance with current UK legislation. Following an incision through the abdomen the portal vein was removed and immediately placed in physiological salt solution (PSS). Freshly dispersed SMCs were liberated using enzymatic digestion, as previously described (Saleh & Greenwood, 2005) and allowed to adhere to a glass base chamber located on the stage of an Axiovert 25 inverted microscope (Carl Zeiss, Germany). Currents were recorded at room temperature (20–22°C) using pCLAMP 9.0 software (Axon Instruments, Union City, CA, USA) and either a List amplifier (HEKA Elektronik, Lambrecht/Pfalz, Germany) or an Axopatch 200B amplifier (Axon Instruments). For all experiments patch pipettes of between 4 and 6 MΩ were pulled by a Narishige PP-830 puller, fire polished and backfilled with the appropriate intracellular solution (see Drugs and solutions). SMCs were identified by their characteristic spindle shaped appearance and were accessed in the perforated patch configuration with amphotericin B. Application of 10 mV hyperpolarising pulses were used to estimate cell size following integration of the evoked capacitive transient, and the mean value was 20.8 ± 1 pF ($n = 18$). Cells were voltage clamped to a holding potential of −60 mV (V_h) unless otherwise indicated and in current clamp mode the amplifier was set to CC + comm (List) or normal current clamp setting (Axopatch).

Tissue retrieval, RNA extraction and RT-PCR

During the tissue retrieval and RNA extraction procedures, precautions were taken to prevent RNAse activity and all surfaces and instruments were cleaned with RNase AWAY (Invitrogen, Carlsbad, CA, USA). Total RNA was extracted following the Qiagen RNeasy minikit protocol for fibrous tissue (Qiagen, Valencia, CA, USA). The extracted RNA was then precipitated using ammonium acetate with linear acrylamide (Ambion, Inc., Austin, TX, USA) as the carrier. RNA was transcribed into cDNA using Superscript II (Invitrogen) according to the manufacturer's protocol using Oligo dt-primers (Invitrogen). Gene specific primers for *SCN1a*, *SCN3a*, *SCN7a*, *SCN8a*, *SCN9a*, *SCN10a*, *SCN11a* and β-actin were designed using Oligoperfect designer software (Invitrogen) whilst primers for *SCN4a* and *SCN5a* were adapted from Zimmer *et al.* (2002) (for primers see Table 1). PCR reactions were carried out in a Touchgene thermocycler (Stratagene, La Jolla, CA, USA). Each PCR reaction contained (final concentration) 5 μl 10× PCR

buffer, 1 μl (0.2 mM) dNTP, 1.5 μl (1.5 mM) $MgCl_2$, 0.5 μl (2.5 units) PlatinumTaq, 1 μl (0.2 μM) of each PCR primer and 1 μl of template DNA made up to 50 μl with water. Amplification was carried out using PlatinumTaq polymerase (Invitrogen) and the protocol involved an initial denaturation at 94°C for 2 min to activate the Taq followed by 35 cycles of denaturing at 94°C for 30 s, annealing at 55°C for 30 s and extension at 72°C. PCR products were loaded onto 1.5% agarose gels made up with 1 × TAE buffer (Invitrogen) containing ethidium bromide (Sigma, Poole, UK) for standard electrophoresis. Gels were visualised on a UVP 3UV transilluminator and photographed using a Kodak Digital Science DC40 instant gel camera. Amplicons were cut out, extracted and purified using the Qiagen QIAquick gel extraction kit. Purified cDNA was ligated into the pGEM-T plasmid vector (Promega Corp., Madison, WI, USA) and transformed using JM109 competent cells (Promega) and grown on Agar plates containing Ampicillin, X-Gal (5-bromo-4-chloro-3-indolyl-β-D-galactopyranoside) and IPTG (isopropyl-β-D-thiogalactopyranoside) for blue/white screening. Plasmids containing inserts were confirmed using a colony lysis PCR. Plasmid DNA was purified using a Qiagen plasmid midi kit and sent for sequencing to the Advanced Biotechnology Centre (Imperial College London, UK).

Immunocytochemistry

Single cells were fixed by 4% paraformaldehyde solution in physiological saline solution (PSS) for 10 min at room temperature and washed with PSS alone. After incubation with PSS containing bovine serum albumin (BSA) and Triton X-100, the cells were incubated with primary antibodies in PSS containing BSA and Triton X-100 overnight at 4°C. To confirm specificity of the antibodies, control experiments were performed where the primary antibodies were preincubated for 15 min with antigenic peptides ($NaV_{1.6}$: CIANH TGVDI HRNGD FQKNG, corresponding to residues 1042–1061 of rat and mouse $NaV_{1.6}$; $NaV_{1.7}$: EFTS IGRSR IMGLS E, corresponding to residues 446–460 of rat $NaV_{1.7}$ and 302–316 of mouse $NaV_{1.7}$ (13 from 15 amino acids)). After this step, the cells were washed and incubated with secondary antibodies conjugated with fluorescent probes. After removing the unbound secondary antibodies by washing the preparations with PSS, single cells were imaged using a laser scanning confocal microscope. The channels were labelled using rabbit polyclonal antibodies against either the voltage-dependent Na^+ channels type 1.6 ($NaV_{1.6}$: dilution 1 : 200) or the type 1.7 ($NaV_{1.7}$: 1 : 200) and were visualised with Alexa Fluor 488 (Molecular Probes, Eugene, OR, USA)-conjugated chicken anti-rabbit antibodies (1 : 500).

All the antibodies were dissolved in deionised water, aliquoted, and kept at −20°C until use. PSS contained penicillin (20 U ml^{-1}) and streptomycin (20 μg ml^{-1}) at all times during immunocytochemical experiments.

Confocal microscopy

The cells were imaged using a Zeiss LSM 510 laser scanning confocal microscope (Carl Zeiss, Jena, Germany). The excitation beam was produced by an argon laser (488 nm) and delivered to the specimen via a Zeiss Apochromat 63× oil immersion objective (numerical aperture 1.4). Emitted fluorescence was captured using LSM 510 software (release 3.2, Carl Zeiss). The cells were scanned in three dimensions as a z-stack of two-dimensional images (512 × 512 pixels) 0.1 μm apart.

Analysis of data

Raw confocal imaging data were processed and analysed using Zeiss LSM 510 software. An image cutting horizontally through approximately the middle of the cell was selected out of a z-stack of images. To assess the cellular distribution of NaV channels, a circular area of 2 μm^2 (diameter approx. 1.6 μm; referred to as Region 1) was randomly selected in the subplasmalemmal area of the cell (Fig. 5*A*) so that its perimeter touched the edge of the cell. Another circular area of 2 μm^2 (Region 2) was selected so that the perimeter of that circle touched the perimeter of Region 1 and the line bisecting these circles was perpendicular to the edge of the cell, thought to be the plasma membrane. A percentage of fluorescing pixels (%FP) was calculated in both regions using the formula

$$\%\mathrm{FP} = 100 \times \frac{n(p > \mathit{threshold})}{n(p)},$$

where $n(p > \mathit{threshold})$ is the number of pixels within the region whose intensity equalled or exceeded the threshold value (usually 10 intensity units (I.U.), to exclude the low intensity pixels caused by photomultiplier noise) and $n(p)$ is the total number of pixels in the region. The percentage FP values were then compared with each other and with the percentage FP in the whole confocal plane of the cell. The average pixel fluorescence (APF) value was used to compare the overall fluorescence signal between the staining and its controls and was calculated using the formula:

$$\mathrm{APF} = \frac{\sum i(p)}{n(p)} (\mathrm{I.U./pixel}),$$

where $i(p)$ is the intensity of a pixel within the confocal plane of the cell and $n(p)$ is the total number of pixels of the plane. Statistical evaluation and graphs were done using Origin software (OriginLab Corp., Northampton,

MA, USA) and final images were produced using CorelDraw 10 software (Corel Corp., Ottawa, Ontario, Canada).

Isometric tension recordings

Portal veins were ligated *in situ* using 3/0 gauge silk braided suture thread (Pearsalls Sutures, Somerset, UK) immediately proximal to the porta hepatis and distal to the anastomosis of splenogastric vein and mesenteric vein. Connective tissue and fat were removed by sharp dissection and the tissue placed in a 10 ml organ bath containing Krebs solution maintained at 37°C and gassed with 95% O_2–5% CO_2 at a resting tension of 0.1 g. Changes in isometric tension were recorded using a BIOPAC Systems Inc. (Goleta, CA, USA) force transducer and Acqknowledge software (version 3.7). All veins were spontaneously active within minutes of arrangement and remained rhythmic for the duration of the experiment. After equilibration for 1 h various sodium channel modulators were applied to the bath. Data were quantified by measuring three different parameters of the spontaneous activity during a 1 min period immediately prior to any intervention. The parameters measured were: peak force generated per individual contraction (*amplitude*), the interval between individual contractions (*interval*) and the duration of individual contractions (*duration*) measured at 10% of the maximum amplitude.

Drugs and solutions

The composition of the dissociation solution was (mM): 125 NaCl, 5.4 KCl, 15.4 $NaHCO_3$, 0.33 Na_2HPO_4, 0.34 KH_2PO_4, 10 glucose, 11 Hepes and 0.1 $CaCl_2$. During electrophysiological recordings cells were perfused with an extracellular PSS containing (mM): 126 NaCl, 1.2 $MgCl_2$, 1.5 $CaCl_2$, 10 glucose and 10 Hepes. This was supplemented with 5 mM KCl for current clamp recordings.

The intracellular solution for voltage clamp perforated patch experiments contained (mM): 126 CsCl, 10 Hepes, 5 EGTA, 4 $MgCl_2$, 5 Na_2ATP (pH set 7.2 with NaOH). For current clamp mode the intracellular solution contained (mM): 130 KCl, 10 Hepes, 5 EGTA, 1 $MgCl_2$, 3 Na_2ATP, 3 MgATP and 0.1 GTP with pH set 7.2 with KOH. In every case electrical responses were obtained using the perforated patch variant of the whole cell technique using amphotericin B. Stock solutions of amphotericin B at 30 mg ml^{-1} were prepared in DMSO that was diluted to the target concentration of 300 μg ml^{-1} every hour. The PSS for the functional experiments was (mM): 125 NaCl, 4.6 KCl, 15.4 $NaHCO_3$, 1 Na_2HPO_4, 2.5 $CaCl_2$, 0.6 $MgSO_4$, 10 glucose. All reagents were purchased from Sigma (Poole, UK) except for collagenase type I (Calbiochem) and KB-R7943 (Tocris Cookson, Bristol, UK). TTX was a kind gift from Professor P. Andrews (St. George's, University of London). The primary antibodies were obtained from Alomone Laboratories (Israel) and the secondary fluorescent antibodies were from Molecular Probes.

Statistics

All data are expressed as mean values ± standard error of the mean (S.E.M.) for the number of cells (n) analysed. Statistical significance was calculated using Student's t test for paired observations unless otherwise stated and differences where $P < 0.05$ were considered significant.

Identity of sequencing data were confirmed using NCBI Blast, Ensembl Blast and retrieved sequences were also directly compared to target sequences using Multalin (http://prodes.toulouse.inra.fr/multalin/multalin.html).

Results

Depolarization of murine portal vein myocytes from a holding potential of −60 mV evoked three different types of response (Fig. 1). In the majority of cells ($n = 192$ or 74%) a slowly activating inward current sensitive to nicardipine was evoked that has been studied in a previous report (Saleh & Greenwood, 2005) and represented the opening of voltage-dependent L-type calcium channels (I_{CaL}, Fig. 1*A*). In 30 cells (16%, see Fig. 1*D*) I_{CaL} had superimposed upon it a more rapidly activating and transient current (termed I_{FAST}) resulting in the generation of a biphasic gross inward current at some test potentials (Fig. 1*B* and *C*). In the remaining 19 cells there was no inward current whatsoever (Fig. 1*D*). When V_h was adjusted to the more negative value of −90 mV the incidence of I_{FAST} appearance increased to 50% (13 from 26 cells). Both depolarization evoked currents could be recorded using the ruptured patch whole cell configuration with the pipette solution containing EGTA. With this configuration 62% of the cells contained I_{CaL} only whilst 20% contained a biphasic current and 18% showed no current ($n = 45$). Consequently, in murine portal vein myocytes depolarization evoked two distinct ionic conductances, I_{CaL} and a more variable I_{FAST}.

Determination of the ionic nature of I_{FAST}

The identity of I_{FAST} was ascertained by the use of pharmacological agents and manipulation of the ionic conditions. I_{FAST} was resistant to the L-type Ca^{2+} channel antagonist nicardipine (1 μM, $n = 6$, Fig. 1*B*), the T-type Ca^{2+} channel antagonist mibefradil (100 μM, $n = 3$, not

shown) and the heavy metal cations Cd^{2+} (1 mM, $n = 3$, Fig. 1*C*) and Ni^{2+} (100 μM, $n = 4$, not shown). These data show that I_{FAST} was not due to the activation of L- or T-type calcium channels. Unlike I_{CaL} I_{FAST} was unaffected by increasing extracellular Ca^{2+} concentration from 1.5 mM to 10 mM (Saleh & Greenwood, 2005), but was abolished when external Na^+ was removed and replaced with equimolar Tris (Figs 2*A* and 3*A*, $n = 5$). In contrast Tris did not have any significant effect on the I_{CaL} component of the biphasic current (Fig. 2*A*, $n = 3$) or on I_{CaL} alone ($n = 3$). These data show that I_{FAST} was carried by Na^+ ions. As voltage-gated Na^+ channels can be broadly separated by their sensitivity to TTX, we investigated the effect of this agent on I_{FAST}. Application of 1 μM TTX inhibited I_{FAST} rapidly and was readily reversed upon washout. Figure 2*B* shows that the effect of TTX was concentration dependent with half-maximal inhibition achieved by 12 ± 1 nM ($n = 4$). Consequently, I_{FAST} was a Na^+ current generated by the voltage-dependent activation of a highly TTX-sensitive Na^+ channel.

Biophysical properties of the voltage gated Na^+ current

In the presence of 1 μM nicardipine I_{FAST} was found to be voltage dependent with a peak amplitude of -80 ± 18 pA around the voltage range of 0–20 mV and a reversal value of +40 mV (Fig. 3). The activation and decay of I_{FAST} were voltage dependent with τ decreasing from 5.7 ± 0.6 ms at −10 mV to 1.6 ± 0.5 ms at +20 mV ($n = 5$, Fig. 3*B*). Steady-state activation and inactivation of the current were assessed using a two-step protocol where the cells were stepped from −60 mV to a range of voltages between −100 and 40 mV for a period of 2 s before a 400 ms step to 0 mV until returning to −60 mV. The values for half-maximal ($V_{0.5}$) inactivation and activation were -52 ± 9 and $+5 \pm 7$ mV, respectively ($n = 4$, Fig. 3*C*).

Molecular biology

To determine the molecular identity of the Na^+ channel isoform, total RNA was extracted as described in Methods

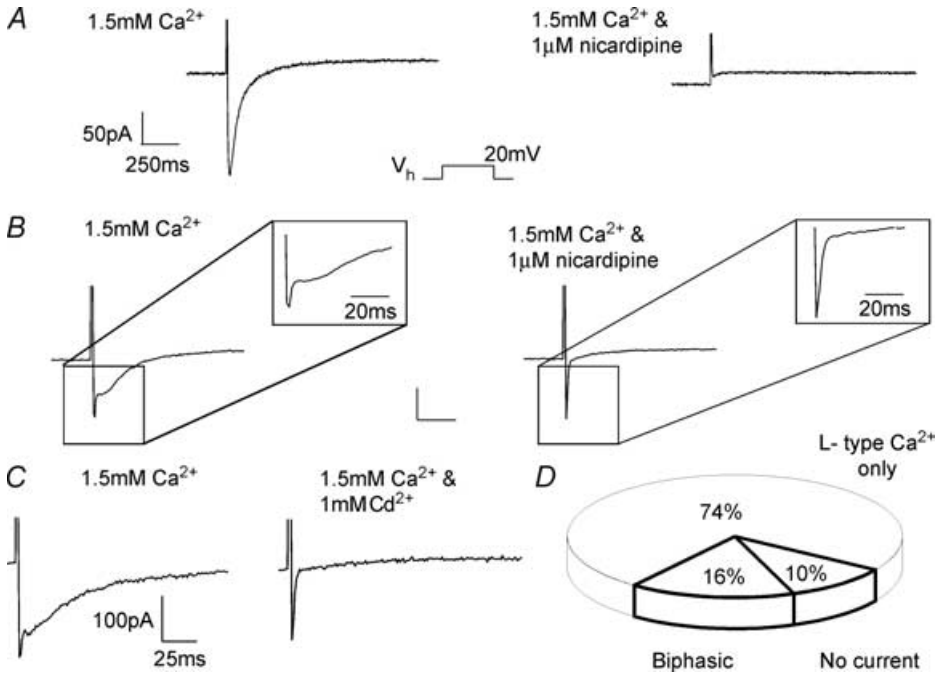

Figure 1. Identification of a 'fast' nicardipine-resistant voltage-dependent current in freshly dissociated murine portal vein smooth muscle myocytes

A, a representative trace of an L-type Ca^{2+} current (I_{CaL}), which was seen in 74% of cells in the voltage clamp mode using the perforated patch configuration. The protocol involved a step from −60 mV to +20 mV and the inward current was abolished by nicardipine (1 μM). *B*, example traces of the currents seen in 16% of cells under identical conditions and using the same protocol described for *A*. The relatively slow I_{CaL} was superimposed on another component that had faster kinetics (I_{FAST}). I_{FAST} was not dihydropyridine-sensitive (1 μM nicardipine) and was not inhibited by 1 mM $CdCl_2$ (*C*). The unlabelled scalars represent 50 pA and 250 ms. *D*, the distribution of current types seen in cells accessed in the perforated patch configuration and voltage clamped at a holding potential of −60 mV. Those with properties similar to *A* were categorised as L-type Ca^{2+} only, whilst waveforms similar to *B* and *C* were considered biphasic. A small percentage of cells also showed no inward current upon depolarization (total $n = 192$).

and RT-PCR was used to probe for transcripts of the Na^+ channels. The specificity of the custom designed primers for *SCN1a*, *3a*, *4a*, *5a*, *7a*, *8a*, *9a* and *11a* were tested on tissues previously shown to express these isoforms. *SCN1a* ($NaV_{1.1}$), *SCN3a* ($NaV_{1.3}$), *SCN8a* ($NaV_{1.6}$) and *SCN9a* ($NaV_{1.7}$) are TTX-sensitive Na^+ channels primarily expressed in the central nervous system. *SCN4a* ($NaV_{1.4}$) is also TTX sensitive and has been shown to be present in the murine heart (Zimmer *et al.* 2002). *SCN5a* ($NaV_{1.5}$) and *SCN11a* ($NaV_{1.9}$) are TTX resistant and are expressed in the heart and peripheral nervous system (PNS), respectively. *SCN7a* (Na_x) has not been shown to form a functional Na^+ channel (for review see Ogata & Ohishi, 2002). Total RNA extracted from mouse brain, heart and portal vein were reverse transcribed into cDNA and positive amplicons for *SCN1a*, *3a*, *7a*, *8a* and *9a* were detected in the mouse brain; *SCN4a*, *5a*, *7a* and *9a* in mouse heart; and *SCN7a*, *8a* and *9a* in the portal vein (Fig. 4). The identities of these amplicons were confirmed by sequencing and bioinformatic analysis. These studies show that the murine portal vein expresses three voltage-gated Na^+ channel genes of which *SCN8a* and *SCN9a* encode for TTX-sensitive products.

Mouse portal vein SMCs stained positive for $NaV_{1.6}$ and $NaV_{1.7}$

Experiments were performed with antibodies specific for the proteins encoded by *SCN8a* ($NaV_{1.6}$) and *SCN9a* ($NaV_{1.7}$) to confirm that these proteins were expressed in single SMCs from the portal vein. Mouse portal vein SMCs stained positive for both $NaV_{1.6}$ ($n = 20$ cells from three mice; Fig. 5*A*) and $NaV_{1.7}$ type of voltage-dependent sodium channel ($n = 13$ cells from two mice; Fig. 5*C*). The fluorescence signals for both types of channel were located within 1.6 μm of the plasma membrane, with very little signal originating in the cytoplasm deeper than this ($NaV_{1.6}$: 60.5 ± 4.8%FP in Region 1 *vs.* 15.6 ± 2.9%FP in Region 2, $P < 10^{-10}$, or 30.0 ± 3.8%FP in the whole confocal plane of the cell, $P < 10^{-9}$, $n = 20$ cells; $NaV_{1.7}$: 43.4 ± 5.3%FP in Region 1 *vs.* 13.3 ± 4.5%FP in Region 2, $P < 2 \times 10^{-5}$, or 15.8 ± 1.6%FP in the whole confocal

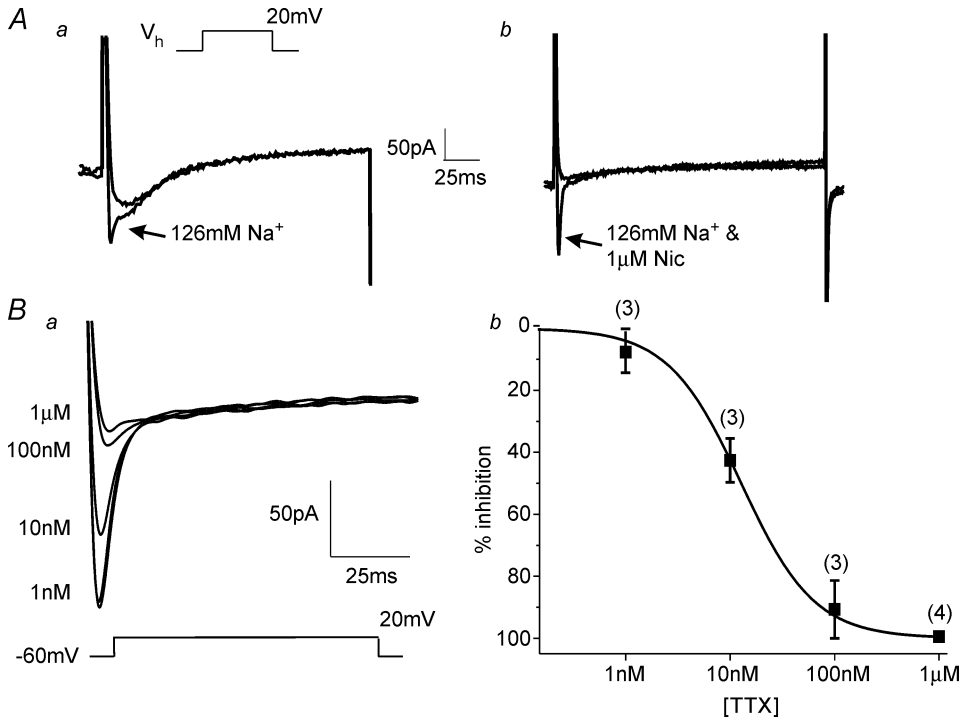

Figure 2. Identification of I_{FAST}
A, the effect of external Na^+ ion replacement by TRIS on biphasic waveforms generated by depolarization from −60 to 20 mV. In *a* the effect is shown on both components of the biphasic waveform whereas *b* shows the effect on a current where the slower I_{CaL} component had been previously removed by application of 1 μM nicardipine (nic). In both incidences the fast component of current was eliminated when the external Na^+ was removed. *Ba*, representative trace from a cell containing I_{FAST} where I_{CaL} has been eliminated by preapplication with nicardipine and the effect of increasing concentrations of tetrodotoxin (TTX) on I_{FAST} amplitude are apparent. *b*, log concentration–effect plot for TTX with the data points fitted with a Hill coefficient and *n* values labelled at each point. The IC_{50} for TTX inhibition was calculated to be 12 ± 1 nM.

plane of the cell, $P < 10^{-4}$, $n = 13$ cells, Fig. 5*E*). The specificity of both antibodies was confirmed by incubation with their respective antigenic peptide (1 : 2 ratio of antibody to antigenic peptide) prior to incubation with the cells, which resulted in almost complete suppression of fluorescence ($NaV_{1.6}$: from 11.1 ± 1.9 I.U. pixel^{-1}, $n = 20$ to 0.7 ± 0.1 I.U. pixel^{-1}, $n = 8$, $P < 0.005$, unpaired t test, Fig. 5*B* and *F*; $NaV_{1.7}$: from 4.7 ± 0.5 I.U. pixel^{-1}, $n = 13$ to 0.3 ± 0.04 I.U. pixel^{-1}, $n = 10$, $P < 10^{-6}$, unpaired t test, Fig. 5*D* and *F*). The control incubations with either primary (not shown) or secondary antibodies alone (Fig. 5*F*, right-most columns in the graph) resulted in virtually no fluorescence (APF < 0.15 I.U. pixel^{-1} in all cases; $NaV_{1.6}$ primary antibodies $n = 7$, $NaV_{1.7}$ primary antibodies $n = 9$, secondary antibodies $n = 8$).

TTX inhibited action potential generation in current clamp mode

In current clamp mode the mean resting membrane potential (V_m) of portal vein (PV) smooth muscle cells was determined to be -54.5 ± 3.5 mV ($n = 18$). In 7 of 12 cells it was possible to generate an action potential (AP) with a current injection of between 50 and 200 pA for 2–3 ms whereas in the remaining cells current injection only resulted in a passive membrane response. This active response took the form of a slowly developing depolarization with a reasonably fast degeneration (see Fig. 6*A*). The mean peak response of the AP with a 2 ms and 75 pA pulse from seven cells was -4.7 ± 3 mV, although an overshoot of +12.3 mV was observed in one cell. In several cases the AP was also accompanied by one or a series of 'after-depolarizations' (Fig. 6*A*). Application of 1 μM TTX resulted in membrane hyperpolarization shifting the V_m from -62 ± 7 mV to -72 ± 5 mV ($n = 3$, $P = 0.1$), whilst also inhibiting the generation of an AP (Fig. 6*Aa*). It was however, possible to generate an AP in the presence of 1 μM TTX but a more substantial current injection was required (Fig. 6*Aa*). However, 2 μM nicardipine abolished AP generation without significantly affecting V_m (-45 ± 9 mV to -47 ± 9 mV, $n = 4$, $P > 0.5$). Figure 6*Ab* shows a typical family of membrane responses to current injections of up to 125 pA from a cell in the absence and presence of 2 μM nicardipine

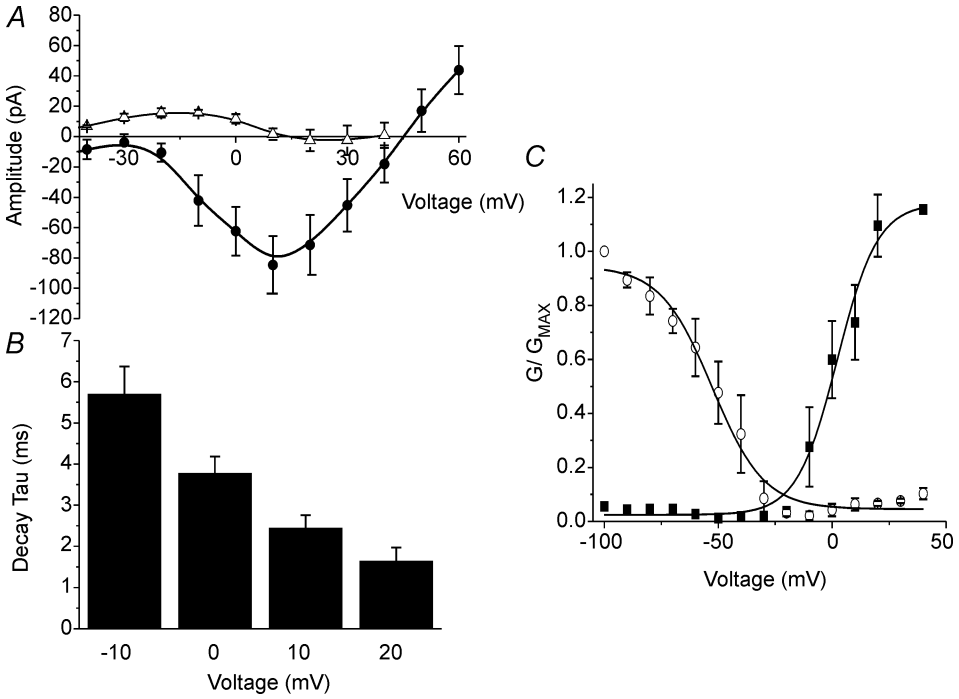

Figure 3. Biophysical properties of I_{FAST}
A, the current–voltage (*I–V*) relationship of I_{FAST} measured at the peak inward current in the presence of 1 μM nicardipine (●) and the corresponding cells in a Na^+ free external solution (△). Removal of Na^+ from the external solution abolished I_{FAST} leaving a small outward current at negative potentials. *B*, a bar graph illustrating the mean voltage dependent deactivation kinetics of I_{FAST} measured at the voltage steps indicated from a $V_h = -60$ mV ($n = 5$) calculated by fitting the data with a single exponential. *C*, the activation and inactivation of the channel in the presence of 1 μM nicardipine. The mean peak current values were established using a double pulse protocol in which cells were stepped from −60 mV to a range of voltages between −100 and +40 mV for 1.5 s, followed by a 250 ms step to +20 mV. Inactivation values (○) and activation (■) were normalised to the maximal evoked current and the mean data fitted with a Boltzmann function. All data are represented as means ± S.E.M.

where it is clear that both the AP and the subsequent after-depolarizations were completely abolished ($n = 4$). AP generation was also dependent on the presence of external Ca^{2+} and in six cells where external Ca^{2+} was 0.1 mM, current injection of up to 300 pA for 4 ms failed to result in an AP (data not shown). These data show that voltage-dependent Na^+ channels influence the generation of APs in murine PV myocytes.

The effect of Na^+ channel modulators on mPV rhythmicity in isometric tissue tension recordings

Mouse portal veins exhibited a number of different patterns of spontaneous contractile activity ranging from single contractions to 'bursts' of multiple contractions. Regardless of the type of activity 1 μM TTX had no effect on the spontaneous contractile activity. The mean amplitude and interval were 0.23 ± 0.06 g and 14.1 ± 2.9 s in the absence and 0.24 ± 0.06 g and 19.3 ± 5.9 s in the presence of TTX ($n = 6$, $P > 0.5$ and $P = 0.19$, respectively, Fig. 6*B*). Application of 5 μM TTX also had no effect on spontaneous contractions of the portal vein (mean amplitude and interval were reduced to 0.19 ± 0.08 g and 20.6 ± 9.8 s, $n = 4$, Fig. 6*B*). In contrast application of the Na^+ channel activator veratridine had marked effects on the spontaneous contractions (see Fig. 7). Thus, 10 μM veratridine caused a significant increase in the interval between individual contractions from 11 ± 2 s to 28.8 ± 3.9 s ($n = 6$, $P < 0.001$) and this was associated with an increase in the duration of each contraction from 7.3 ± 1.8 s to 19 ± 3.5 s ($P = 0.003$). Whilst there was an increase in amplitude in some tissues this was not supported statistically (0.19 ± 0.02 g and 0.21 ± 0.02 g in the absence and presence of 10 μM veratridine, respectively. The effects of 50 μM veratridine were even more marked (see Fig. 7*A*). The intercontraction interval increased from 9.9 ± 2.3 s to 35.2 ± 4.2 s ($P < 0.001$) and the contraction duration increased from 5.6 ± 1.2 s to 27 ± 5 s ($n = 6$, $P = 0.004$). The effects of veratridine were apparent immediately after application of 50 μM veratridine to the bath but took between 3 and 5 min to reach a steady state. The veratridine product was ablated instantly upon application of 1 μM TTX in the continued presence of veratridine (see Fig. 7*A*). Interestingly the amplitudes of the spontaneous contractions in the presence of veratridine and TTX (0.07 ± 0.01 g) were significantly less than contractions recorded before application of veratridine (0.11 ± 0.02 g, $P < 0.05$, $n = 5$). The veratridine effect was not inhibited by a 5 min preincubation with guanethedine (30 μM) or a combination of 5 μM atropine, 5 μM propranolol and 5 μM prazosin (Fig. 7*B*) suggesting that it was not the product of transmitter release from adrenergic and cholinergic nerves. The intercontraction interval still increased from 8 ± 0.4 s to 36.3 ± 2.6 s ($P = 0.03$) and the contraction duration from 5 ± 0.1 s to 23.2 ± 0.1 s ($P < 0.001$, $n = 3$). Each of these reagents independently had no significant effect on the portal vein contractility (Fig. 7*B*). The augmented contractile activity induced by veratridine application was, however, dependent on Ca^{2+} entry through L-type Ca^{2+} channels as the contractions were completely abolished by both removal of external Ca^{2+} (not shown) and the application of 1 μM nicardipine (Figs 7*C*, $n = 5$). These data show that functional Na^+ channels are present in whole portal vein smooth muscle and these channels have a marked impact on contractility.

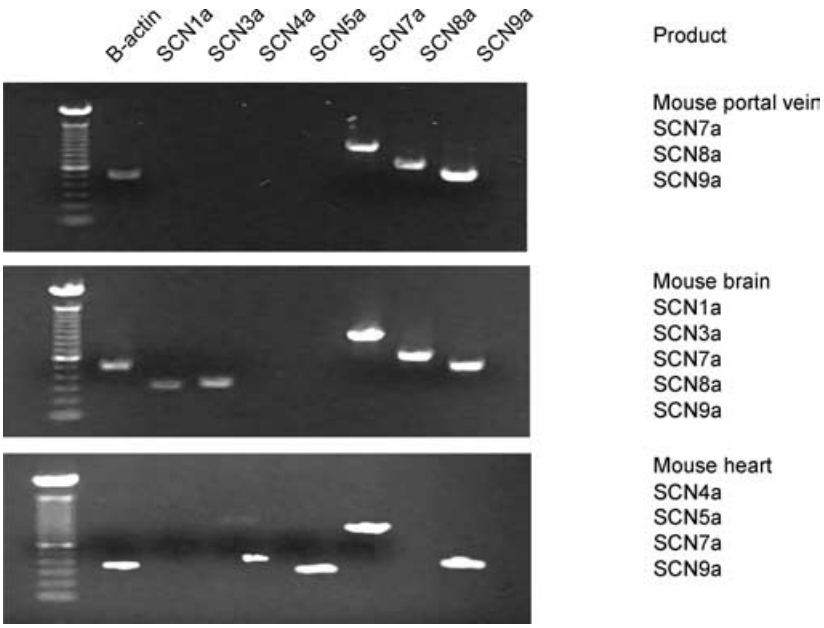

Figure 4. Molecular identification of voltage- dependent Na^+ channel subunits expressed in murine portal vein
Reverse transcriptase polymerase chain reaction was undertaken using primers specific for SCNa isoforms and mRNA extracted from freshly dissected mouse heart, brain and portal vein. The bands have been visualised on a UV trans-illuminator using ethidium bromide incorporated into agarose gels. Positive signals for each Na^+ channel isoform detected are included in the accompanying text.

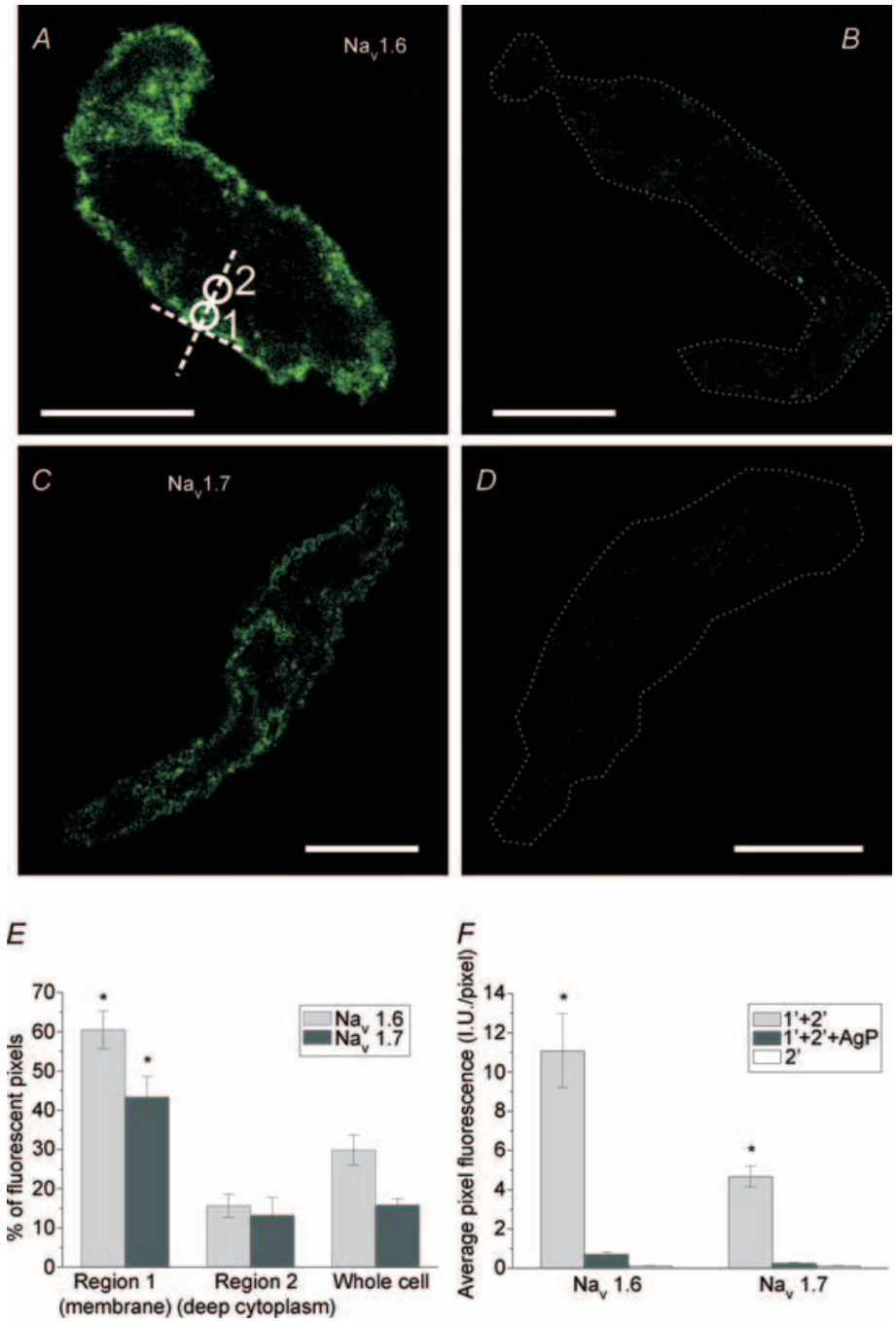

Figure 5. Immunocytochemical staining of murine portal vein smooth muscle cells for $Na_{V1.6}$ and $Na_{V1.7}$ type of voltage-dependent sodium channels

The fluorescence images of a single confocal plane of the cell are labelled with $NaV_{1.6}$ antibodies (*A*); $NaV_{1.6}$ antibodies preincubated with their antigenic peptide (*B*); $NaV_{1.7}$ antibodies (*C*); and $NaV_{1.7}$ antibodies preincubated with their antigenic peptide (*D*). Circles in *A* indicate Regions 1 and 2 that were used to analyse the localization of fluorescence (for details see Methods). The calibration in *A*–*D* is 10 μm. A dotted line has been used in *B* and *D* to outline the contour of a cell, due to its low fluorescence. *E*, the summarized data on localization of $NaV_{1.6}$ and $NaV_{1.7}$ fluorescence in the cells. There was significantly more fluorescence in the region within ~1.6 μm of plasma membrane (Region 1) than in the deep cytoplasm (Region 2) or when compared with whole cell average. *F*, summary data on intensity of fluorescence, expressed as average pixel fluorescence (intensity units per pixel). The values of all pixels in the cell's confocal plane were added up and then divided by the number of such pixels. The specificity of labelling was confirmed for both antibodies by greatly reduced fluorescence after preincubation with respective antigenic peptide or by virtual lack of fluorescence in the absence of primary antibodies. *Statistical significance.

A putative role for the Na^+–Ca^{2+} exchanger in the veratridine response

Recent studies have revealed that Na^+ influx through non-selective cation channels generates marked increases in intracellular Ca^{2+} ($[Ca^{2+}]_i$) by enhancing reverse mode Na^+–Ca^{2+} exchange (Rosker *et al.* 2004; Zhang *et al.* 2005). We therefore instigated a final series of experiments to determine whether the enhanced contractility produced by veratridine may be due to enhanced Ca^{2+} influx via the Na^+–Ca^{2+} exchanger. These experiments revealed that the stimulatory effects of veratridine were nullified by preincubation in 10 μM of KB-R7943, an inhibitor of reverse mode Na^+–Ca^{2+} exchange (Iwamoto *et al.* 1996). In the presence of KB-R7943 the mean intercontraction interval and contraction duration were 7.34 ± 0.59 s and 5.04 ± 0.34 s, respectively ($n = 8$, $P > 0.05$), which were no different from control values (6.98 ± 0.5 s and 4.39 ± 0.28 s). As Fig. 8*A* shows, the contraction interval and duration after application of 50 μM veratridine in the continued presence of KB-R7943 were statistically similar to values recorded in the absence of veratridine. Intriguingly veratridine applied in the continued presence of KB-R7943 induced a small but significant decrease in contraction amplitude from 0.10 ± 0.01 g to 0.08 ± 0.01 g ($n = 8$, $P = 0.04$). Since KB-R7943 has been reported to directly inhibit Na^+ channels in cardiac cells with an IC_{50} of 14 μM (Watano *et al.* 1996) we investigated the possibility that the effect of 10 μM KB-R7943 was exerted by a direct influence on Na^+ channels. Application of 10 μM KB-R7943 reduced the amplitude of the Na^+ current evoked by step depolarization from −90 mV to 0 mV from -194 ± 47 pA to -179 ± 65 pA ($n = 4$, $P = 0.6$, Fig. 8*B*). With this in mind the data suggest that in portal vein activation of TTX-sensitive Na^+ channels enhanced contractility through an involvement of reverse mode Na^+–Ca^{2+} exchange.

Discussion

The present study has shown that a TTX-sensitive Na^+ current is present in freshly dissociated smooth muscle cells from the portal vein and the Na^+ channel gene

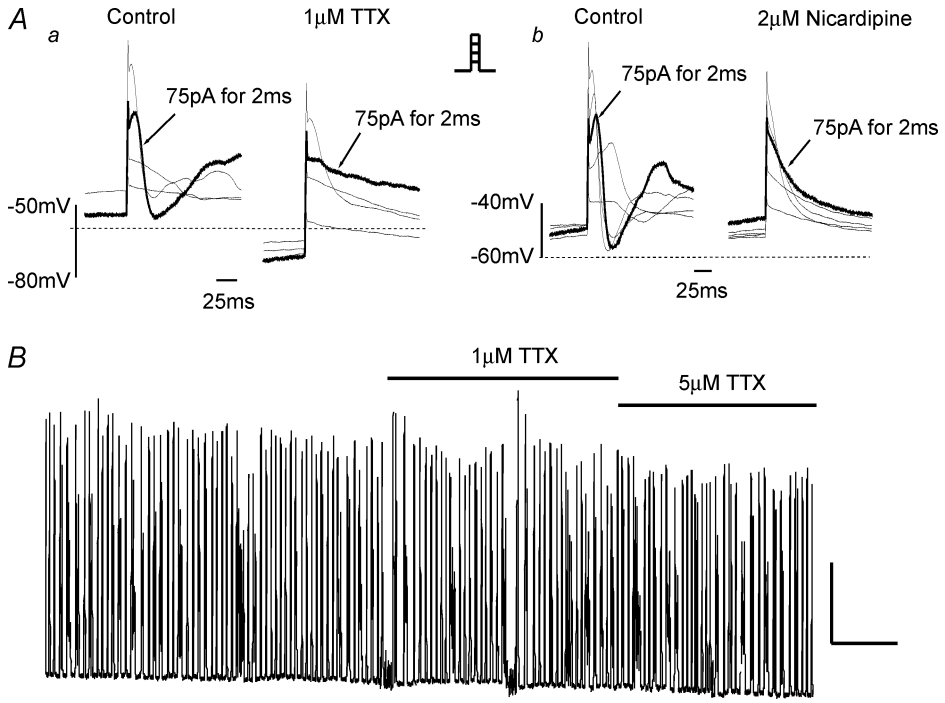

Figure 6. Effect of TTX on action potential generation and portal vein rhythmicity
Aa, representative family of voltage responses generated by applying 2 ms pulses of current in 25 pA increments (see inset) on a cell held in the current clamp mode. The bold trace is indicative of a control (as labelled) action potential (AP) generated by applying 75 pA for 2 ms. Membrane potentials elicited by this protocol in the presence of 1 μM TTX are shown in the right-hand panel. The highlighted trace is the voltage response evoked by 2 ms injection of 75 pA. *Ab*, another family of currents generated under the same conditions using the protocol previously described. Upon application of 2 μM nicardipine (right-hand panel) it was no longer possible to generate an AP even with a 125 pA injection of current. This effect was consistently reproducible ($n = 4$). *B*, a representative isometric tension recording from whole murine portal vein where each vertical deflection represents a spontaneous increase in tension. TTX at 1 and 5 μM was applied for the period denoted by the horizontal bars and had no significant effect on the spontaneous contractions of the portal vein. Unlabelled scalars represent 75 mg and 2 min.

isoforms *SCN7a*, *SCN8a* and *SCN9a* can be detected in total RNA extracted from the portal vein tissue. To determine whether these genes were translated into proteins we used immunocytochemical methods and found the proteins $NaV_{1.6}$ and $NaV_{1.7}$ (corresponding to *SCN8a* and *SCN9a*, respectively) in a predominantly plasmalemmal location. Current clamp studies in isolated individual SMCs were conducted to determine whether Na^+ channels were able to influence AP generation and revealed that 1 μM TTX attenuated evoked APs, which was still dependent on Ca^{2+} entry through L-type Ca^{2+} channels. Further studies were conducted on whole PV in isometric tension tissue bath recordings to determine whether these channels played any role in the spontaneous rhythmicity of the portal vein. Surprisingly, the TTX-sensitive Na^+ channels did not seem to be involved in the generation or maintenance of the rhythmicity but they were able to play a modulatory role through an indirect mechanism apparently involving reverse mode Na^+–Ca^{2+} exchange. These data revealed for the first time the molecular identity of voltage-dependent Na^+ channels in non-cultured freshly dissociated smooth muscle cells.

Electrophysiological characterization

While trying to characterise $I_{Cl(Ca)}$ currents evoked by Ca^{2+} entry through VDCCs (Saleh & Greenwood, 2005) a second current was found superimposed upon the L-type Ca^{2+} current (I_{CaL}). This current had much faster activation and deactivation kinetics relative to I_{CaL} and was resistant to the T-type Ca^{2+} channel blockers Cd^{2+}, Ni^{2+} and mibefridil. However, similar to Na^+ currents in guinea pig ureter (Muraki *et al.* 1991), rabbit pulmonary artery (Okabe *et al.* 1988), rat vas deferens (Belevych *et al.* 1999) and human oesophagus (Deshpande *et al.* 2002) the fast current in the portal vein was very sensitive to TTX with an IC_{50} of 12 ± 1 nM (Fig. 3*Bb*). The abolition of I_{FAST} upon external Na^+ ion replacement provided further evidence that this current arose as a result of inward Na^+ ion movement (Figs 2*A* and 3*A*). The VGSCs in murine portal vein SMCs had a $V_{0.5}$ inactivation value of −52 ± 9 mV and this value was similar to VGSCs seen in various smooth muscle cell types (Mironneau *et al.* 1992; Hollywood *et al.* 1997; Yoshino *et al.* 1997; Deshpande *et al.* 2002; Holm *et al.* 2002). Thus voltage-gated Na^+ currents in murine portal vein myocytes had very similar biophysical properties to those recorded in other cell types.

Molecular biology

Whilst VGSCs have been recorded from a number of smooth muscle cells there is very little information on their molecular identity. To date a TTX-resistant Na^+ current was shown in jejunal circular muscle from morbidly obese humans and the tissue was found to express *SCN5a*, *10a* and *11a* (Holm *et al.* 2002; Ou *et al.* 2002). Alternatively cultured cells from the oesophagus and various arteries exhibiting a TTX-sensitive Na^+ channel were found to express *SCN4a* and *6a* by Deshpande *et al.* (2002; oesophagus) or *SCN3a*, *5a* and *9a* by Jo *et al.* (2004; vascular tissues). However, no real conclusions can be drawn from these studies as it could be argued that the Na^+ channel genes detected were a result of pathophysiological

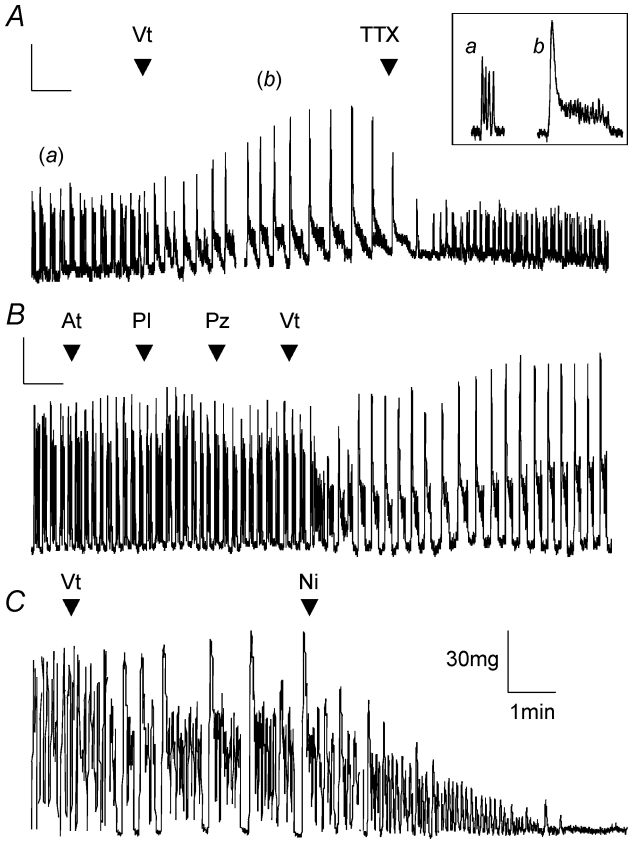

Figure 7. Analysis of the effect of veratridine on whole portal veins
A, representative trace from an isometric tension recording showing the effect of veratridine, which significantly altered the contraction frequency, the duration of contraction and the interval between contractions in all tissues (see text, $n = 6$). These effects were reversed by the application of 1 μM TTX ($n = 5$). The inset shows a magnification of the sections indicated. The scalars represent 50 mg and 2 min for the long-term trace and 100 mg and 30 s for the inset. *B*, trace showing the effects of applying 5 μM atropine (At), 5 μM propranolol (Pl) and 5 μM prazosin (Pz) to the PV. The effect of veratridine (Vt) was not affected by preincubation with these reagents demonstrating that it was independent from cholinergic or adrenergic influence. Similar effects were observed in 2 other tissues. The scalars represent 30 mg and 3 min. *C*, the effect of 50 μM veratridine on spontaneous contractions under the same conditions as the previous traces. In this example application of 1 μM nicardipine not only reversed the veratridine product but also resulted in an almost complete abolition of all contractions.

circumstances (Holm *et al.* 2002; Ou *et al.* 2002) or due to the cell culturing procedure (Deshpande *et al.* 2002; Jo *et al.* 2004). To address these specific issues we conducted our studies on tissues freshly excised from healthy adult mice. Therefore the discovery of a Na^+ current and evidence of VGSC isoform expression was indicative of their presence in a normal physiological scenario. In the murine portal vein we detected the Na^+ channel gene isoforms *SCN7a*, *8a* and *9a* and this represents the first identification of VGSC gene expression in healthy and non-cultured smooth muscle.

However, the existence of mRNA does not necessarily mean the existence of a translated product, i.e. the protein. For that reason immunocytochemical studies were carried out on freshly dispersed portal vein SMCs using antibodies generated to specifically detect a short amino acid sequence unique to the $NaV_{1.6}$ (*SCN8a*) and $NaV_{1.7}$ (*SCN9a*) proteins. *SCN7a* has not been shown to form a functional VGSC and was therefore excluded. The polyclonal antibodies generated to detect the $NaV_{1.6}$ and $NaV_{1.7}$ subunits showed positive fluorescence on the individual myocytes (Fig. 5*A* and *B*). This fluorescence was blocked by prior incubation with control antigens thus confirming specific staining. The staining pattern showed predominantly plasmalemmal staining with the $NaV_{1.6}$ channel giving a stronger signal than the $NaV_{1.7}$ channel (Fig. 5*E* and *F*).

Functional studies on $NaV_{1.6}$ and $NaV_{1.7}$

There is some doubt as to whether *SCN7a* encodes a functional Na^+ channel, but a number of studies have shown the expression of *SCN8a* and *9a* genes yields TTX-sensitive Na^+ channels. The *SCN8a* gene is localised on chromosome 12 of the mouse genome and is predominantly expressed in the central nervous system where it is one of the most abundant voltage gated sodium channels (Caldwell, 2000). The $NaV_{1.6}$ protein was identified as the major channel in the nodes of Ranvier of myelinated axons (Caldwell *et al.* 2000; Krzemian *et al.* 2000) and plays a major role in the conduction of neural impulses with mutations resulting in muscle weakness (Sprunger *et al.* 1999) tremor, ataxia (Smith & Goldin, 1998) and paralysis (Meisler *et al.* 2004). Smith *et al.* (1998) showed that a full-length construct of the mouse *SCN8a* gene expressed in *Xenopus* oocytes gave a functional TTX-sensitive Na^+ channel with an IC_{50} of 6.4 ± 0.6 nM. The current resulting from *SCN8a* expression had a $V_{0.5}$

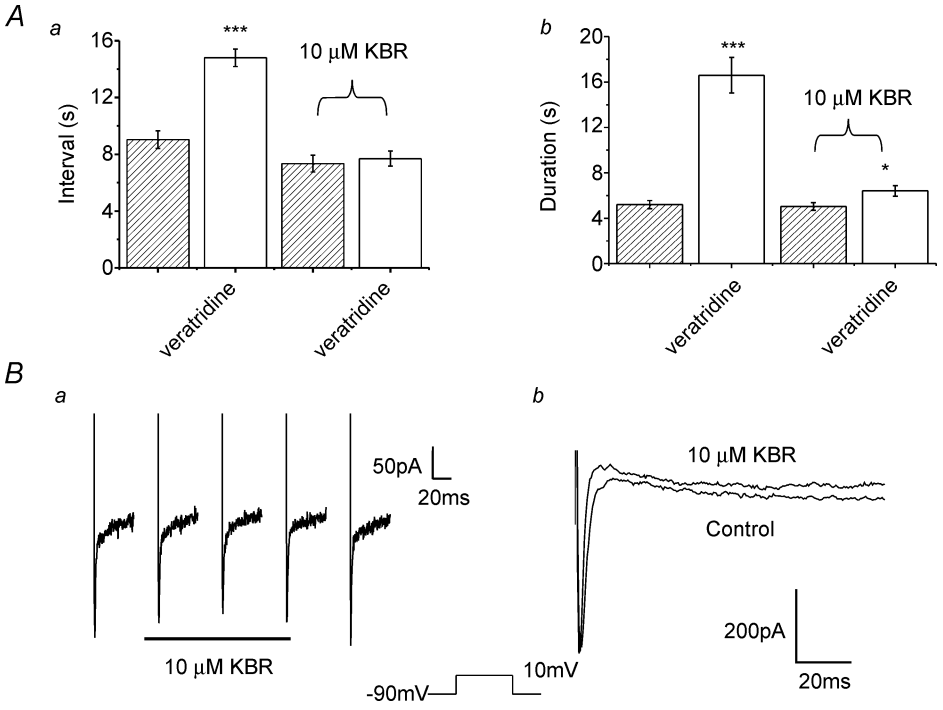

Figure 8. The effects of K- BR7943
A, bar charts representing mean data (± S.E.M., $n = 8$) showing the effect of veratridine on the interval between contractions (*a*) and the duration of contractions (*b*) under normal conditions and following 10 min of preincubation with the reverse mode Na^+–Ca^{2+} exchange blocker KB-R7843 (10 μM as labelled). *B*, the effect of 10 μM KB-R7943 (KBR) on I_{FAST} evoked by depolarization from −90 mV (as labelled). *a*, traces showing the decrease in I_{FAST} amplitude upon application of KBR and the subsequent increase upon washout. *b*, an example of a cell where KBR did not inhibit I_{FAST} amplitude but this agent increased the apparent decay of the evoked current.

for inactivation of -55 ± 3 mV and a $V_{0.5}$ for activation of -8.8 ± 4 mV when *SCN8a* was expressed alone, whilst these values were -51 ± 1 mV and -17 ± 4 mV when coexpressed with the genes for Na^+ channel β_1 and β_2 subunits. These biophysical characteristics of *SCN8a* are strikingly similar to those of the native Na^+ current seen in the portal vein.

The *SCN9a* gene has been mapped to the proximal segment of the mouse chromosome 2 and forms part of a cluster of four *SCNa* genes (*SCN1a*, *2a*, *3a* and *6a*, Beckers *et al.* 1996). The corresponding $NaV_{1.7}$ channel is expressed primarily in the sensory and sympathetic neurones of the PNS and is known to play an important role in nociception (Nassar *et al.* 2004; Wood *et al.* 2004). Transient transfection of HEK293 cells with this gene produced a rapidly activating and inactivating current with a current density of about 65 pA pF^{-1} that reached maximal amplitude at -10 mV. The current had a $V_{0.5}$ for inactivation of -60.5 ± 1.6 mV and an IC_{50} for TTX sensitivity of 24.5 nM. The biophysics of the expressed channel was only slightly affected by coexpression with the β_1 subunit and it was also able to induce action potentials in the HEK293 cells (Klugbauer *et al.* 1995). The finding of *SCN8a* and *SCN9a* expression in the murine portal vein suggests that the classification of these Na^+ channel genes as neuronal may not be entirely accurate.

Functional role of VGSC

APs generated in isolated cells in the current clamp mode were inhibited by 1 μM TTX, which was also found to reduce membrane excitability by causing hyperpolarization. This was similar to findings by Amédée *et al.* (1986), Muraki *et al.* (1991) and Hollywood *et al.* (1997) who all showed that evoked APs were blocked by TTX, although the former two required excessively high concentrations of TTX (10 μM). However, unlike Hollywood *et al.* (1997) the mouse PV cells' AP was also abolished by an L-type Ca^{2+} channel blocker (Fig. 6*A*) and was dependent on extracellular Ca^{2+}. Our data on PV myocytes bears considerable resemblance to the work of Muraki *et al.* (1991) who reported that in the rat stomach fundus and guinea pig ureter SMC contraction was dependent on Ca^{2+} influx predominantly through dihydropyridine-sensitive Ca^{2+} channels but the generation of APs was influenced by the opening of Na^+ channels.

Since murine portal veins are spontaneously active and this activity has been shown to be dependent on Ca^{2+} influx through dihydropyridine-sensitive Ca^{2+} channels (Spencer & Greenwood, 2003; Saleh & Greenwood, 2005) there seemed to be sufficient evidence to suggest that Na^+ channels may play an integral role in this phenomenon. However, spontaneous activity of the whole tissue was not affected by concentrations of TTX that abolished the Na^+ current and inhibited the AP in smooth muscle cells. Thus, unlike the TTX-sensitive electrically induced contractions in isolated sheep lymphatic rings (Hollywood *et al.* 1997), VGSCs do not appear to be involved in the inherent contractility of portal veins in the isometric conditions employed in the present study. In this preparation, however, veratridine (10–50 μM), which removes the inactivation intrinsic to VGSCs (Sutro, 1986), had a significant effect on the portal vein spontaneous rhythmicity, causing increases in both the interval between contractions and the duration of each contraction. Furthermore this effect was reversed by the Na^+ channel blocker TTX (1 μM, Fig. 7*A*). These results were very similar to those seen by Amédée *et al.* (1986) in rat myometrial tissue, who also found that TTX (10 μM) inhibited APs in isolated smooth muscle cells but failed to do so on intact tissue strips, which were shown to be dependent on extracellular Ca^{2+}. Further investigation by this group found that sea anemone toxin II, which has a similar mechanism of action to veratridine, augmented APs in a Ca^{2+}-independent but TTX-sensitive manner (Amédée *et al.* 1986). In the mouse PV we found that the veratridine effect was not due to the release of transmitters from cholinergic or adrenergic nerves as the response was unaffected by preincubation in guanethedine or a cocktail containing atropine, propranolol and prazosin. However, the removal of external Ca^{2+} (data not shown) and the application of nicardipine abolished all activity proving that the veratridine product was still dependent on Ca^{2+} influx through dihydropyridine-sensitive channels. Comparable effects were also reported by Shinjoh *et al.* (1991) who observed that veratridine and batrachotoxin induced contractions in rat aorta, a tissue ordinarily quiescent. They also found that this effect was blocked by TTX and was dependent on Ca^{2+} influx. Overall, the whole tissue experiments prove that whilst VGSCs are present in murine portal veins they appear not to be involved in the initiation and maintenance of the mouse PV spontaneous activity. This suggests that the spontaneous mechanical activity is driven by cells, be they specialised pacemaker cells (ICC-like) or a subset of smooth muscle cells, which do not rely on VGSCs. However activation of these channels can augment the inherent contractile activity of the PV. As numerous membrane receptors and intracellular signals affect the activity of these proteins (e.g. Wada *et al.* 2004) the role of VGSCs in this preparation may be dependent on the underlying physiological status.

A possible role for the Na^+–Ca^{2+} exchanger

Recent experiments have revealed that Ca^{2+} entry through the Na^+–Ca^{2+} exchanger working in reverse mode can be stimulated by Na^+ influx through TRP cation channels (Rosker *et al.* 2004) and this mechanism underlies proliferation in pulmonary artery myocytes (Zhang *et al.* 2005). Moreover, Na^+ loading of single

myocytes from rabbit portal vein increased $[Ca^{2+}]_i$ sufficiently to activate Ca^{2+}-dependent Cl^- channels (Leblanc & Leung, 1995). Therefore we speculated that the increased contractility produced by veratridine might have emanated from reverse mode Na^+–Ca^{2+} exchange driven by a VGSC-generated increase in $[Na^+]_i$. Consequently, we studied the effect of KB-R7943, an isothiourea derivative that preferentially inhibits the reverse mode of Na^+–Ca^{2+} exchange (Iwamoto *et al.* 1996), on the stimulatory effect of veratridine. KB-R7943 had no effect on spontaneous activity itself but prohibited the veratridine-induced increase in contractility. This affect is unlikely to be due to direct blockade of the VGSC by KB-R7943 as reported previously (Watano *et al.* 1996) as 10 μM KB-R7943 caused a nominal and statistically insignificant decrease of the Na^+ current in PV myocytes. These findings suggest that opening of VGSC in PV myocytes is capable of influencing the Na^+–Ca^{2+} exchanger analogous to the scenario reported in cardiomyocytes (Leblanc & Hume, 1990).

Conclusion

Although we have shown that Na^+ channels exist in mouse PV myocytes and can have a functional contribution we can only hypothesise about their exact role much like other groups have before us in different preparations (Muraki *et al.* 1991; Shinjoh *et al.* 1991). However, we have established for the first time the molecular identity of VGSC in freshly dispersed, healthy smooth muscle cells and have not only shown that the mRNA signals for the TTX-sensitive Na^+ channel subtypes *SCN8a* and *SCN9a* are present in the PV but also that into their corresponding protein products $NaV_{1.6}$ and $NaV_{1.7}$ are present on individual cells.

References

Amédée T, Renaud JF, Imari K, Lombet A, Mironneau J & Lazdunski M (1986). The presence of Na^+ channels in myometrial smooth muscle cells is revealed by specific neurotoxins. *Biochem Biophys Res Commun* **137**, 675–681.

Beckers MC, Ernst E, Belcher S, Howe J, Levenson R & Gros P (1996). A new sodium channel alpha-subunit gene (SCN9A) from Schwann cells maps to the SCN1A, SCN2A, SCN3A cluster of mouse chromosome 2. *Genomics* **36**, 202–205.

Belevych AE, Zima AV, Vladimirova IA, Hirita H, Jurkiewicz A, Jurkiewicz NH & Shuba MF (1999). TTX-sensitive Na^+ and nifedipine-sensitive Ca^{2+} channels in rat vas deferens smooth muscle cells. *Biochim Biophys Acta* **1419**, 343–352.

Caldwell JH (2000). Clustering of sodium channels at the neuromuscular junction. *Micros Res Tech* **49**, 84–89.

Caldwell JH, Schaller KL, Lasher RS, Peles E & Levinson SR (2000). Sodium channel $Na_v1.6$ is localized at nodes of Ranvier, dendrites and synapses. *Proc Natl Acad Sci U S A* **97**, 5616–5620.

Deshpande MA, Wang J, Preiksatis HG, Laurier LG & Sims SM (2002). Characterisation of voltage-dependent Na^+ current in human oesophageal smooth muscle. *Am J Physiol* **283**, C1045–C1055.

Hollywood MA, Cotton KD, Thornbury KD & McHale NG (1997). Tetrodotoxin-sensitive sodium current in sheep lymphatic smooth muscle. *J Physiol* **15**, 13–20.

Holm AN, Rich A, Miller SM, Strege P, Ou Y, Gibbons S *et al.* (2002). Sodium current in human jejunal circular smooth muscle cells. *Gastroenterology* **122**, 178–187.

Iwamoto T, Watano T & Shigekawa M (1996). A novel isothiourea derivative selectively inhibits the reverse mode of Na^+/Ca^{2+} exchange in cells expressing NCX1. *J Biol Chem* **271**, 22391–22397.

Jo T, Nagata T, Iada H, Imuta H, Iwasawa K, Ma J *et al.* (2004). Voltage-gated sodium channel expressed in cultured human smooth muscle cells: involvement of SCN9A. *FEBS Letts* **567**, 339–343.

Klugbauer N, Lacainova L, Flockerzi V & Hofmann F (1995). Structure and functional expression of a new member of the tetrodotoxin-sensitive voltage-activated sodium channel family from human neuroendocrine cells. *EMBO J* **14**, 1084–1090.

Krzemian DL, Schaller KL, Levinson SR & Caldwell JH (2000). Immunolocalization of sodium channel isoform NaCh6 in the nervous system. *J Comp Neurol* **420**, 70–83.

Leblanc N & Hume JR (1990). Sodium current-induced release of calcium from cardiac sarcoplasmic reticulum. *Science* **248**, 372–376.

Leblanc N & Leung PM (1995). Indirect stimulation of Ca^{2+}-activated Cl^- current by Na^+/Ca^{2+} exchange in rabbit portal vein smooth muscle. *Am J Physiol Heart* **268**, H1906–H1917.

Meisler MH, Plummer NW, Burgess DL, Buchner DA & Sprunger LK (2004). Allelic mutations of the sodium channel SCN8a reveal multiple cellular and physiological functions. *Genetica* **122**, 37–45.

Mironneau J, Martin C, Arnadeau S, Imari K, Rakotoarisoa L, Sayet I *et al.* (1990). High affinity binding sites for [^{3}H]saxitoxin are associated with voltage-dependent sodium channels in portal vein smooth muscle. *Eur J Phamacol* **184**, 315–319.

Muraki K, Imaizumi Y & Watanabe M (1991). Sodium currents in smooth muscle cells freshly isolated from stomach fundus of the rat and ureter of the guinea pig. *J Physiol* **442**, 351–375.

Nassar MA, Stirling LC, Forlani G, Baker MD, Matthews EA, Dickenson AH *et al.* (2004). Nociceptor-specific gene deletion reveals a major role for $Na_V1.7$ (PN1) in acute and inflammatory pain. *Proc Natl Acad Sci U S A* **101**, 12706–12711.

Ogata N & Ohishi Y (2002). Molecular diversity and function of the voltage-gated Na^+ channels. *Jpn J Pharmacol* **88**, 365–377.

Okabe K, Kitamura K & Kuriyama H (1988). The existence of a highly tetrodotoxin-sensitive Na channel in freshly dispersed smooth muscle cells of the rabbit main pulmonary artery. *Pflugers Arch* **411**, 423–428.

Ou Y, Gibbons S, Miller SM, Strege P, Rich A, Distad MA *et al.* (2002). SCN5a is expressed in human jejunal circular smooth muscle cells. *Neurogastroenterol Motil* **14**, 477–486.

Rosker C, Graziani A, Lukas M, Eder P, Zhu MX, Romanin C *et al.* (2004). Ca^{2+} signaling by TRPC3 involves Na^+ entry and local coupling to the Na^+/Ca^{2+} exchanger. *J Biol Chem* **279**, 13696–13704.

Saleh SN & Greenwood IA (2003). Characterisation of calcium-activated chloride currents in murine smooth muscle myocytes. *J Physiol* **552**, C3.

Saleh SN & Greenwood IA (2005). Activation of chloride currents in murine portal vein smooth muscle cells by membrane depolarization involves intracellular calcium release. *Am J Physiol Cell Physiol* **288**, C122–C131.

Shinjoh M, Nakaki T, Otsuka Y, Sasakawa N & Kato R (1991). Vascular smooth muscle contraction induced by Na^+ channel activators, veratridine and batrachotoxin. *Eur J Pharmacol* **205**, 199–202.

Smith MR & Goldin AR (1998). A mutation that causes ataxia shifts the voltage-dependence of the SCN8a sodium channel. *Neuroreport* **10**, 3027–3031.

Smith MR, Smith RD, Plummer NW, Meisler MH & Goldin AL (1998). Functional analysis of the mouse SCN8a sodium channel. *J Neurosci* **18**, 6093–6102.

Spencer NJ & Greenwood IA (2003). Characterisation of properties underlying rhythmicity in mouse portal vein. *Auton Neurosci* **104**, 73–82.

Sprunger LK, Escayg A, Tallaksen-Greene S, Albin RL & Meisler MH (1999). Dystonia associated with mutation of the neuronal sodium channel SCN8a and identification of the modifier locus Scnm1 on mouse chromosome 3. *Hum Molec Genet* **8**, 471–479.

Sturek M & Hermsmeyer K (1986). Calcium and sodium channels in spontaneously contracting vascular smooth muscle cells. *Science* **233**, 475–478.

Sutro JB (1986). Kinetics of veratridine action on Na channels of skeletal muscle. *J General Physiol* **87**, 1–24.

Wada A, Yanagita T, Yokoo H & Kobayashi H (2004). Regulation of cell surface expression of voltage-dependent $Na_V1.7$ sodium channels: mRNA stability and post-traanslational control in adrenal chromaffin cells. *Frontiers Bioscience* **9**, 1954–1966.

Watano T, Kimura J, Morita T & Nakanishi H (1996). A novel antagonist, 7943, of the Na^+/Ca^{2+} exchange current in guinea-pig cardiac ventricular cells. *Br J Pharmacol* **119**, 555–563.

Wood JN, Boorman JP, Okuse K & Baker MD (2004). Voltage-gated sodium channels and pain pathways. *J Neurobiol* **61**, 55–71.

Yoshino M, Wang SY & Kao CY (1997). Sodium and calcium inward currents in freshly dissociated smooth myocytes of rat uterus. *J General Physiol* **110**, 565–577.

Zhang S, Yuan JX, Barrett KE & Dong H (2005). Role of Na^+/Ca^{2+} exchange in regulating cytosolic $[Ca^{2+}]$ in cultured human pulmonary artery smooth muscle cells. *Am J Physiol Cell Physiol* **288**, C245–C252.

Zimmer T, Bollensdorff C, Haufe V, Birch-Hirschfeld E & Benndorf K (2002). Mouse heart Na^+ channels: primary structure and function of two isoforms and alternatively spliced variants. *Am J Physiol Heart Circ Physiol* **282**, H1007–H1017.

Acknowledgements

Work in I.A.G.'s and S.A.P.'s laboratories is supported by the British Heart Foundation (BHF), the Biotechnology and Biological Sciences Research Council (BBSRC) in association with GlaxoSmithKline (GSK) and the Wellcome Trust grant 042293. V.P. is a BHF intermediate research fellow (FS/04/052). The authors would like to thank Dr D. Trezise (GSK), Dr M. Main (Astra-Zeneca) and Professor Paul Andrews (SGHMS) for their input and Alomone Laboratories for their kind gift of the $NaV_{1.7}$ antibody.